International Journal of
Molecular Sciences

MDPI

Article

Multichromosomal Mitochondrial Genome of *Paphiopedilum micranthum*: Compact and Fragmented Genome, and Rampant Intracellular Gene Transfer

Jia-Xing Yang [1], Nicolas Dierckxsens [2], Ming-Zhu Bai [1] and Yan-Yan Guo [1,*]

[1] College of Plant Protection, Henan Agricultural University, Zhengzhou 450046, China
[2] Center for Human Genetics, KU Leuven, 3000 Leuven, Belgium
* Correspondence: guoyy@henau.edu.cn

Abstract: Orchidaceae is one of the largest families of angiosperms. Considering the large number of species in this family and its symbiotic relationship with fungi, Orchidaceae provide an ideal model to study the evolution of plant mitogenomes. However, to date, there is only one draft mitochondrial genome of this family available. Here, we present a fully assembled and annotated sequence of the mitochondrial genome (mitogenome) of *Paphiopedilum micranthum*, a species with high economic and ornamental value. The mitogenome of *P. micranthum* was 447,368 bp in length and comprised 26 circular subgenomes ranging in size from 5973 bp to 32,281 bp. The genome encoded for 39 mitochondrial-origin, protein-coding genes; 16 tRNAs (three of plastome origin); three rRNAs; and 16 ORFs, while *rpl10* and *sdh3* were lost from the mitogenome. Moreover, interorganellar DNA transfer was identified in 14 of the 26 chromosomes. These plastid-derived DNA fragments represented 28.32% (46,273 bp) of the *P. micranthum* plastome, including 12 intact plastome origin genes. Remarkably, the mitogenome of *P. micranthum* and *Gastrodia elata* shared 18% (about 81 kb) of their mitochondrial DNA sequences. Additionally, we found a positive correlation between repeat length and recombination frequency. The mitogenome of *P. micranthum* had more compact and fragmented chromosomes compared to other species with multichromosomal structures. We suggest that repeat-mediated homologous recombination enables the dynamic structure of mitochondrial genomes in Orchidaceae.

Keywords: Orchidaceae; slipper orchid; hybrid assembly; multichromosomal genome; intracellular gene transfer

Citation: Yang, J.-X.; Dierckxsens, N.; Bai, M.-Z.; Guo, Y.-Y. Multichromosomal Mitochondrial Genome of *Paphiopedilum micranthum*: Compact and Fragmented Genome, and Rampant Intracellular Gene Transfer. *Int. J. Mol. Sci.* **2023**, *24*, 3976. https://doi.org/10.3390/ijms24043976

Academic Editor: Abir U. Igamberdiev

Received: 26 January 2023
Revised: 11 February 2023
Accepted: 13 February 2023
Published: 16 February 2023

1. Introduction

The mitochondrion is a key organelle involved in a series of cellular processes. Angiosperm mitochondrial genomes (mitogenomes) are characterized by a low mutation rate, a highly dynamic genome structure, extensive variation in genome size, long non-coding regions, frequent recombination, RNA editing, and widespread horizontal gene transfer [1–7]. For instance, the smallest mitogenome is found in the hemiparasitic *Viscum scurruloideum*, with a length of 66 kb [8], whereas the mitogenome of *Silene conica* has expanded to 11.3 Mb [9]. Earlier studies have indicated that plant mitogenomes exist as circular structures. However, there is increasing evidence that the genomic conformation of mitogenomes can be more complex than just one circular structure. Electron micrographs of the mitochondria of *Chenopodium album* have shown a subgenome that is circular with a linear tail [10], while some species even show a complex branched structure [11], and a multichromosomal structure has been independently identified in multiple lineages [3,9,11–19]. For example, the mitogenome of *S. conica* consists of 128 circular chromosomes ranging in size from 44 kb to 163 kb [9]. The number of mitochondrial chromosomes ranges from 2 in multiple species to 132 in *Picea glauca* [17]. Furthermore, the mitochondrial genes have shown a disparity in their substitution rates [20–22], and the synonymous substitution rate in *Ajuga* has shown a 340-fold

range [20]. In contrast, *Liriodendron tulipifera* has a "fossilized" mitochondrial genome, which has undergone little change over the last 100 million years [23].

Angiosperm mitogenomes are poorly characterized compared to their plastomes or to animal mitogenomes (NCBI database, 351 land plants mitogenomes, 13 July 2022) and are dominated by species from the crop families, such as Brassicaceae, Fabaceae, Poaceae, and Solanaceae [24]. In addition, the complexity of mitogenome assembly is exacerbated by their multichromosomal structure, recombination, lengthy repeat sequences in intergenic spacer regions and introns, and horizontal gene transfer events [11]. For instance, the intron of *cox2* expanded to 11.4 kb in *Nymphaea colorata*, and the repeat sequences accounted for 49% of its mitogenome [25]. The total length of repeat sequences in *S. conica* even reaches 4621 kb and accounts for 40.8% of the mitogenome [9]. Repeat-mediated homologous recombinations have resulted in different conformations coexisting in the same species [19,25–30]. In some cases, the long, plastid-like sequences will lead to erroneous extensions that produce chimeric contigs comprising both mitogenomic and plastomic sequences [31]. With the rapid advances in long-read sequencing technologies and assembly methods, long repeat regions and plastid-derived fragments in the plant mitogenomes [32,33] can now be resolved, which will facilitate the study of angiosperm mitogenomes.

Orchidaceae is one of the largest families of angiosperms, with about 28,000 species (World Checklist of Orchidaceae). All orchids depend on mycorrhizal fungi for seed germination in their initial stage of development, and many orchids rely on mycorrhizal fungi for nutrients in their later life [34–36]. The symbiotic relationship between orchids and fungi makes orchids an outstanding candidate for investigating the evolution of mitogenomes. There has only been one draft-assembled mitogenome of Orchidaceae reported to date: the mitogenome of holo-heterotrophic *Gastrodia elata*, consisting of 19 contigs (13.5 kb to 410.3 kb) with a total length of 1340 kb, which is one of the largest mitogenomes of angiosperms sequenced, to date [37]. Further, there are six other orchid species from the subfamily Epidendroideae with multichromosomal structures available in GenBank (unpublished data). The general features of a mitogenome from other clades of Orchidaceae are unknown. Considering the large species number in this family, the mitogenome evolution of orchids needs more case studies. Furthermore, previous studies have shown widespread intracellular gene transfer or horizontal gene transfer, including plastome-to-mitogenome gene transfer, mitogenome-to-nuclear gene transfer, and horizontally transferred foreign sequences in the mitogenome obtained from unrelated plant species [3,12,16,23,31,38–45]. Zhao et al. [38] summarized that the mitochondrion is the source of horizontal gene transfer. For instance, the mitogenome of *Amborella trichopoda* contains entire mitogenomes from three green algae and one moss [3]. Choi et al. [41] identified non-retroviral endogenous RNA viral elements (NERVEs) and transposable elements across legume mitogenomes. Further, the symbiosis between orchids and fungi likely boosts the opportunities for horizontal gene transfer between them. Moreover, Sinn and Barrett [31] found two ancient horizontal transfer events between orchids and fungi: one 270 bp fragment encoding three tRNA genes obtained from the mitogenome of fungi and the other > 8 kb fragment encoding 14 genes from a fungal mitogenome to the mitogenome of ancestors of the subfamily Epidendroideae. Further, Sinn and Barrett [31] speculated that the horizontal events involving plant mitogenomes might be underestimated, owing to the lack of completely sequenced genomes. However, the work of Sinn and Barrett [31] did not cover species from the subfamily Cypripedioideae.

In this study, we report the sequencing, assembling, and annotation of the mitogenome of *Paphiopedilum micranthum* using a combination of Illumina and PacBio sequencing platforms. *P. micranthum* is a species that was first described in 1951; it is known as the "silver slipper orchid", has high ornamental value, and is distributed from the north of Vietnam to the southwest of China [46]. We aimed to decipher the structure and gene content of the mitogenome of *P. micranthum* and compare the *P. micranthum* mitogenome with the *G. elata* mitogenome. Furthermore, we wanted to assess the intracellular gene transfer between the plastome and mitogenome of *P. micranthum*, and test the horizontal gene transfer between the mitogenome and fungi detected by Sinn and Barrett [31]. Finally, we calculated the

recombination frequency of the repeat pairs and tested the relation between repeat length and the recombination frequency.

2. Results

2.1. The Multichromosomal Structure of the P. micranthum Mitogenome

The mitogenome of *P. micranthum* was assembled into 26 circular chromosomes with lengths ranging from 5973 bp to 32,281 bp, with a total length of 447,368 bp (Figure 1). The average GC content of the *P. micranthum* mitogenome was 44.4%, ranging between 40.4% and 49.2% among chromosomes (Table 1). We obtained, for most of the chromosomes, a sequencing depth above 40× for the long reads and 500× for the short reads (Table S1). Both long- and short-read assemblies were almost identical, except for Chr5 (20,211 bp), which existed as one circular sequence in the short-read sample and fragmented into Chr5A (9033 bp) and Chr5B (11,178 bp) in the long-read sample. Both minicircles were supported by 32 and 102 long reads, respectively (Figure S1). The mitogenome of *P. micranthum* encoded 70 genes, including 39 mitochondrial protein-coding genes, 12 plastome-derived protein-coding genes, 16 tRNA genes, and three rRNA genes (rrn5, rrn18, and rrn26) (Figure 2, Table 2). Further, 16 ORFs coding for hypothetical proteins with BLAST hits were preserved (Figure 1, Tables 2 and S2). In addition to the copy of rrn5 on Chr2, which is identical to the one annotated in *G. elata* [37], the copy on Chr22 was truncated at the 5′ end (88 bp) and relatively shorter than the normal one. Each chromosome had one to four genes, whereas Chr18, with a length of 14,612 bp, was devoid of functional genes (Figure 1). Further, the "empty" sequence presented no significant similarities to the sequences in GenBank.

Most of the mitochondrial genes had a conserved gene length, whereas some genes varied greatly in length, e.g., *atp6* expanded to 1272 bp, *atp9* expanded to 327 bp, *sdh4* contracted to 204 bp (Table S3), and these three genes underwent RNA editing according to the prediction in PREPACT. Furthermore, we identified 25 Group II introns, including 19 cis-spliced introns and six trans-spliced introns, located in seven cis-splicing genes (*ccmFc*, *cox2*, *nad4*, *nad7*, *rpl2*, *rps3*, and *rps10*) and three trans-splicing genes (*nad1*, *nad2*, and *nad5*) (Figure 1, Tables 2 and S4). The exons of *nad1*, *nad2*, and *nad5* were encoded on different chromosomes (Figure 1). For *nad5*, the five exons of *nad5* separated across three chromosomes, with exon1 and exon2 in Chr8, exon3 in Chr12, and exon4 and exon5 in Chr1 (Figure 1).

The tRNAs of *P. micranthum* came from different origins, including twelve native mitochondrial-origin tRNAs (*trnE-UUC*, *trnF-GAA*-mt, *trnfM-CAU*, *trnI-CAU*×2, *trnK-UUU*, *trnM-CAU*-mt, *trnP-UGG*×2, *trnQ-UUG*, *trnS-UGA*, and *trnY-GUA*), three plastid-origin tRNAs (*trnF-GAA*-cp, *trnM-CAU*-cp, and *trnN-GUU*), and one bacteria-origin tRNAs (*trnC-GCA*) [42]. The plastome-originating tRNA, *trnF-GAA*-cp, had been reported before in angiosperm mitogenomes [42]. Notably, the mitogenome encoded both *trnF-GAA*-mt (74 bp) and *trnM-CAU*-mt (73 bp) from the mitochondrial origin, and *trnF-GAA*-cp (73 bp) and *trnM-CAU*-cp (73 bp) from the plastome origin. *trnI-CAU* and *trnP-UGG* had duplicated copies in the mitogenome and *trnI-CAU* duplicated in different chromosomes (Chr3 and Chr21), whereas *trnP-UGG* dispersed duplicated in Chr5 (Figure 1). In addition, Chr5 retained a truncated remnant of the plastome-origin *trnV-UAC* (Figure 1). However, some ancient plastome-to-mitogenome tRNAs (e.g., *trnH-GUG* and *trnW-CCA*) that appear in most sequenced angiosperm mitogenomes were not detected, which revealed that the mitogenome of *P. micranthum* experienced gene loss and gain.

Further, gene synteny analyses indicated that the mitogenome of *P. micranthum* retained eight of the 14 ancestral gene clusters reported across angiosperms [23], including *atp4-nad4L*, *rpl2-rps19-rps3-rpl16*, *rpl5-rps14-cob*, *rps13-nad1*.x2.x3, *rrnS-rrn5*, *trnfM(CAU)-rrnL*, *trnF(GAA)-trnP(UGG)*, and *trnY(GUA)-nad2*.x3.x4.x5.

Figure 1. Map of the *Paphiopedilum micranthum* mitogenome. The genome consisted of 26 circular chromosomes. Genes drawn inside and outside each circle are transcribed clockwise and counter-clockwise. Two triangles show the positions of the overlapping of *cox3-sdh4* and *rpl16-rps3*, with the length of overlap indicated.

Table 1. General features of the mitogenome of *Paphiopedilum micranthum*.

Genome Feature	*Paphiopedilum micranthum*
Genome size (bp)	447,368
Numbers of contigs	26
Contig length	5973 to 32,281
GenBank Nos	OP465200–OP465225
GC content (%)	40.4% to 49.2%
Length of the coding region (%)	40,029 (8.95%)
Length of rRNA genes (%)	5563 (1.24%)
Length of tRNA genes (%)	1206 (0.27%)
Length of cis-spliced introns (%)	27,985 (6.26%)
length of the plastid-derived sequence (%)	46,273 (10.34%)
Number of protein-coding genes (native)	39
Number of protein-coding genes (plastid derived)	12
Number of rRNA genes	3
Number of tRNA genes (native)	13
Number of tRNA genes (plastid derived)	3
Total genes	70

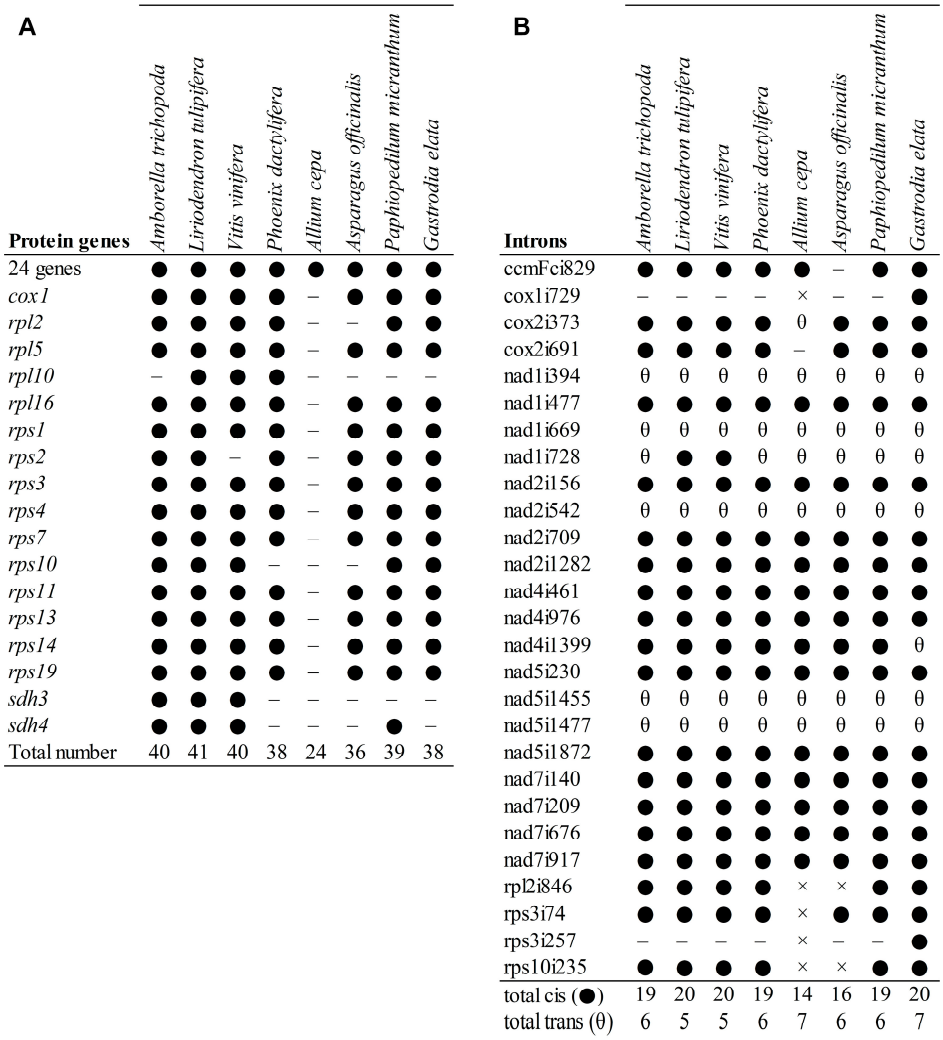

Figure 2. Comparison of the protein-coding gene content and group II intron content of *Paphiopedilum micranthum* and selected angiosperms. (**A**) protein-coding gene content. • indicates present, – indicates lost; the 24 genes present in all sampled species include *atp1*, *atp4*, *atp6*, *atp8*, *atp9*, *ccmB*, *ccmC*, *ccmFc*, *ccmFn*, *cob*, *cox2*, *cox3*, *matR*, *mttB*, *nad1*, *nad2*, *nad3*, *nad4*, *nad4L*, *nad5*, *nad6*, *nad7*, *nad9*, and *rps12*. (**B**) group II intron content. • indicates cis-spliced intron present, – intron lost, θ trans-spliced intron present, × intron loss due to gene loss.

Table 2. Gene content of the mitogenome of *Paphiopedilum micranthum*.

Chromosome	Length (bp)	GC Content (%)	Genes of Mitochondrial Origin	Genes of Chloroplast Origin	ORF
Chr1	32,281	42.2	*nad5* exon 4, *nad5* exon 5, *nad9*	*cemA*, ψ*ndhD*, *petA*, ψ*psaA*, ψ*psaC*, *rbcL*, ψ*rpl14*, ψ*rpl16* fragment, *ycf4*, *trnF-GAA*-cp	ORF102a, ORF116, ORF128
Chr2	28,701	43.1	*rrn5*, *rrn18*	ψ*ndhE* fragment, ψ*ndhF* fragment, ψ*ycf1* fragment, *trnN-GUU*	ORF149, ORF669
Chr3	24,176	46.8	*nad7*, *trnI-CAU*	—	ORF102b, ORF104, ORF124
Chr4	22,131	42.7	*cob*, *rpl5*, *rps14*	ψ*petB* fragment, ψ*petD* fragment, *rpoA*, ψ*rps11*, *rpl36*, ψ*infA*	
Chr5	20,211	45.3	*matR*, *nad1* exon 5, *trnF-GAA*-mt, *trnP-UGG* (2)	—	
Chr6	20,166	43.1	*atp1*, *atp4*, *ccmFn*, *nad4L*	—	
Chr7	19,839	47.2	*mttB*, *rpl2*, *rpl16*, *rps3*, *rps13*, *rps19*, *nad1* exon 2, *nad1* exon 3, *nad*1 exon 4	—	ORF152
Chr8	19,478	43.1	*nad5* exon1, *nad5* exon2, *trnE-UUC*, *trnS-UGA*, *cox3*, *sdh4*	ψ*accD*, *ndhJ*, ψ*ndhK*, ψ*ndhC*	ORF111
Chr9	19,019	45.8	*cox1*	ψ*rpl2*	
Chr10	18,957	46.1	*nad2* exon 3, *nad2* exon 4, *nad2* exon 5, *trnY-GUA*	ψ*ndhH*, ψ*atpB*, *psbJ*, *psbL*, *psbF*, *psbE*	ORF119
Chr11	18,916	42.2	*atp9*, *rps7*, *trnK-UUU*	ψ*rpoB* fragment, ψ*rpoC1*	
Chr12	18,871	43.9	*ccmC*, *rps2*, *rps4*, *nad5* exon3	ψ*psbA* fragment	
Chr13	17,666	44.6	*ccmFc*	ψ*psbN*, ψ*psbH*, ψ*petB* fragment, ψ*psbB* fragment, ψ*rps8* fragment	
Chr14	16,774	44.9	*nad2* exon1, *nad2* exon2, *trnC-GCA*	—	
Chr15	15,892	43.3	*nad1* exon1	*atpE*, ψ*trnV-UAC* fragment, *trnM-CAU*-cp	
Chr16	15,572	46.1	*cox2*, *rps10*	ψ*matK* fragment	ORF109
Chr17	15,327	49.2	*nad4*	—	ORF165
Chr18	14,612	41.2	—	—	ORF261, ORF432, ORF603
Chr19	13,988	45.5	*rrn26*, *trnfM-CAU*-mt	—	
Chr20	13,709	45.8	*nad3*, *nad6*, *rps11*	—	
Chr21	13,165	45.4	*atp6*, *trnI-CAU*	—	
Chr22	12,852	46.3	*rrn5* fragment, *trnM-CAU*	ψ*atpA* fragment	
Chr23	11,459	43.2	*rps12*, *trnQ-UUG*	—	
Chr24	11,240	44.9	*rps1*	—	
Chr25	6393	40.4	*ccmB*	ψ*rps4*	
Chr26	5973	42.2	*atp8*	ψ*ycf1* fragment	

2.2. Horizontal Gene Transfer or the Intracellular Gene Transfer in the Mitogenome of *P. micranthum*

A total of 15 of the 26 chromosomes in the mitogenome of *P. micranthum* contained plastome-origin sequences, encoding 12 intact protein-coding genes, 3 tRNAs, and 29 pseudogenes (Tables 2 and 3). All of these genes were identified by the plastome of *P. micranthum*, except for ψ*ndhE*, ψ*ndhF,* and ψ*ndhH*, which were identified by the plastome of *Cypripedium tibeticum*. However, the 270 bp fungal mitogenomic region identified by Sinn and Barrett [31] was not detected in the mitogenome of *P. micranthum*. The 25 plastome-derived fragments ranged from 165 bp to 7269 bp, with a total size of 46,273 bp, accounting for 10.34% of the whole mitogenome length and 28.32% of the *P. micranthum* plastome (Figure 3, Table 3). Even the smallest chromosome (Chr26—5973 bp) contained a 903 bp plastome-derived sequence. Most of the plastome-derived sequences showed high similarity to their conspecific plastome sequence (ranging from 84.2% to 99.6%) (Table 3), and 12 of the plastome origin genes were intact and potentially functional, including *ycf4*, *cemA*, *petA,* and a shortened *rbcL* (1047 bp) in Chr1; *rpoA* and *rpl36* in Chr4; *ndhJ* in Chr8; *psbE*, *psbF*, *psbJ*, and *psbL* in Chr10; and a shortened *atpE* (345 bp) in Chr15 (Tables 2 and 3). Particularly, *psbE*, *psbF*, and *trnM-CAU-cp* retained an identical copy with the plastome sequence of *P. micranthum*. However, other plastome-derived genes appeared as pseudogenes, e.g., ψ*ndhD*, ψ*psaA*, ψ*psaC*, and ψ*rpl14* in Chr1; and ψ*atpI*, ψ*ndhE*, ψ*ndhF*, and ψ*ycf1* in Chr2 (Tables 2 and 3). Further, the chromosomes with plastome-origin fragments (40.4% to 46.3%) had lower GC content compared to chromosomes without plastome-origin sequences (41.2% to 49.2%), e.g., the GC content of Chr17 was 49.2%, while the GC content of Chr25 was 40.4% (Table 2).

Table 3. Plastid-derived regions in the mitochondrial genome of Paphiopedilum micranthum.

Chromosome	Length (bp)	Position	Genes Contained	Identity (%)
Chr1	1862	6022–7883	ψ*psaC*–ψ*ndhD*	95.50
Chr1	256	11,166–11,421	none	99.60
Chr1	7269	16,713–23,981	*petA*–*cemA*–*ycf4*–ψ*psaA*	95.90
Chr1	1024	26,693–27,716	ψ*rpl14*–ψ*rpl16*	88.50
Chr1	1549	28,034–29,582	*rbcL*	95.20
Chr1	426	(31,892–32,281) + (1–36)	*trnF(GAA)*	85.20
Chr2	165	5–169	none	94.80
Chr2	1357	19,699–21,055	ψ*ndhE* fragment–ψ*ndhF* fragment	93.00
Chr2	1583	21,146–22,728	ψ*ycf1* fragment–*trnN(GUU)*	91.50
Chr4	4719	157–4875	ψ*petB* fragment–ψ*petD* fragment–*rpoA*–ψ*rps11*–*rpl36*–ψ*infA*	92.30
Chr8	3976	12,854–16,829	ψ*accD*–*ndhJ*–ψ*ndhK*–ψ*ndhC*	93.80
Chr9	1320	11,951–13,270	ψ*rpl2*	96.40
Chr10	415	4673–5087	none	90.90
Chr10	4310	5152–9461	ψ*ndhH*–ψ*atpB*–*psbJ*–*psbL*–*psbF*–*psbE*	93.60
Chr11	1749	566–2314	ψ*rpoB* fragment	87.40
Chr11	4823	9374–14,196	ψ*rpoB* fragment–ψ*rpoC1*	92.60
Chr12	947	1515–2461	ψ*psbA* fragment	92.20
Chr13	2179	400–2578	ψ*psbN*–ψ*psbH*–ψ*petB* fragment–ψ*psbB* fragment	92.50
Chr13	230	3792–4021	ψ*rps8* fragment	88.30
Chr15	1552	(14,959–15,892) + (1–618)	*atpE*–*trnM(CAU)*–ψ*trnV(UAC)* fragment	90.90
Chr16	729	11,631–12,359	ψ*matK* fragment	84.20
Chr22	587	8861–9447	ψ*atpA* fragment	88.30
Chr23	203	10,708–10,910	none	85.80
Chr25	2140	(4328–6393) + (1–74)	ψ*rps4*	84.20
Chr26	903	3032–3934	ψ*ycf1* fragment	89.40

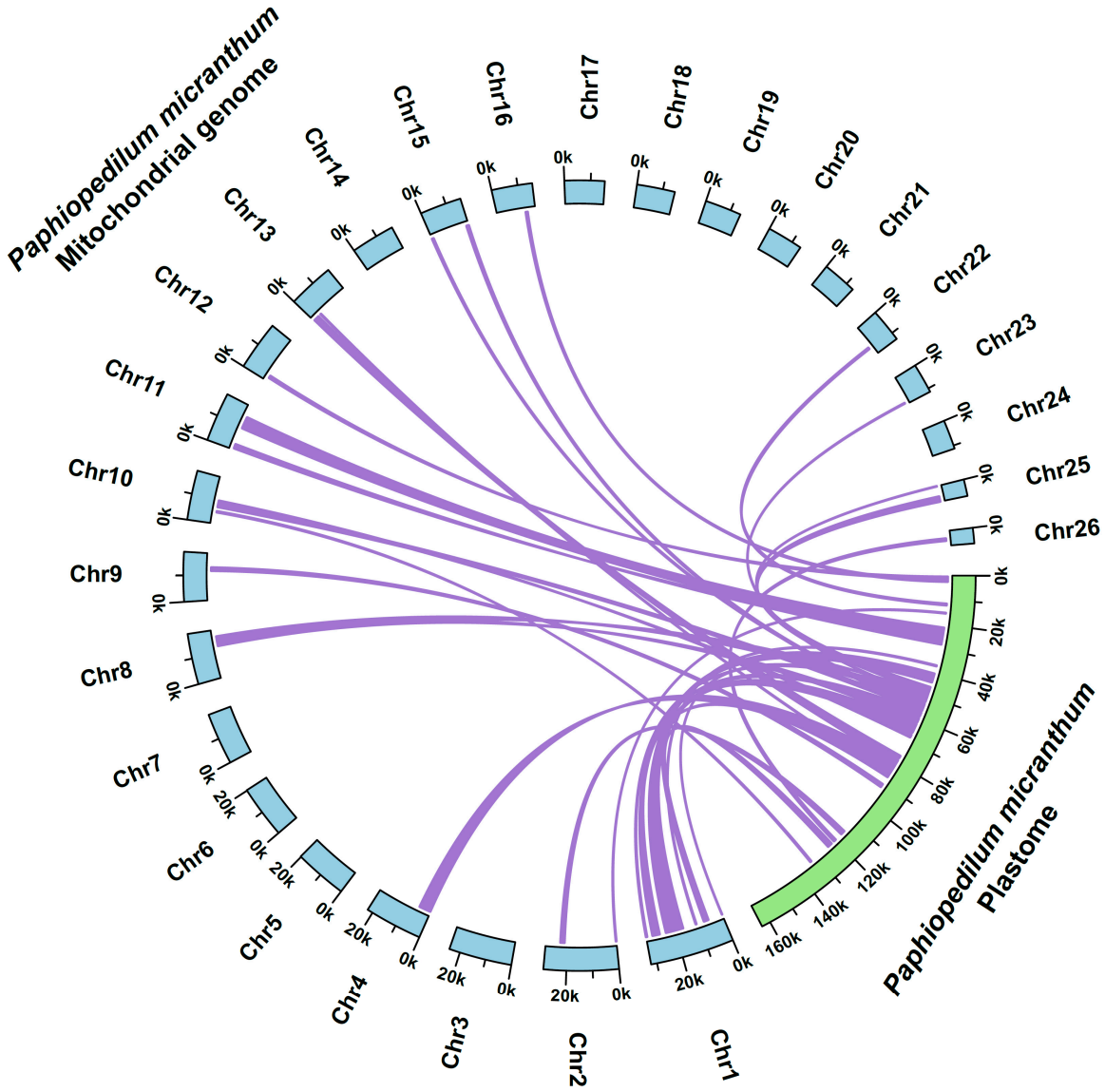

Figure 3. Schematic diagram of gene transfer between the plastome and mitogenome of *Paphiopedilum micranthum*.

2.3. Repeat Sequences in the Mitogenome of P. micranthum

Overall, 27 tandem repeats, with lengths ranging from 27 bp to 308 bp, accounted for 1948 bp of the *P. micranthum* mitogenome; these repeats resided in the non-coding regions of the genome, except for a 48 bp repeat in *rrn26*, and some of the tandem repeats overlapped with the dispersed repeats. The mitogenome of *P. micranthum* possessed 89 dispersed repeats (34 types), ranging from 51 bp to 672 bp, with two to four copies and covering 9996 bp (2%) of the genome. The majority of these repeats (87 of 89, 97.7%) were intermediate-sized repeats (50 to 500 bp) and two repeats (672 bp) were large repeats (>500 bp) (Table S5), with most of these repeats residing in the noncoding regions. These repeats were distributed in 23 of the 26 chromosomes; Chr12, Chr25, and Chr26 did not contain dispersed repeats (Figure 4A). We found 16 pairs of repeats involved in the recombination of the mitogenome structure. The alternative conformations were supported by the long reads, and repeat length was positively correlated with the recombination frequency ($r = 0.9379$, $p < 0.001$), e.g., the recombination frequency of the longest repeat (672 bp) was 0.38; 116 long reads supported the alternative conformations, and 193 long reads supported the master circle

conformation, while homologous recombination occurred sporadically among repeats shorter than 300 bp (Figure 4B, Table S5).

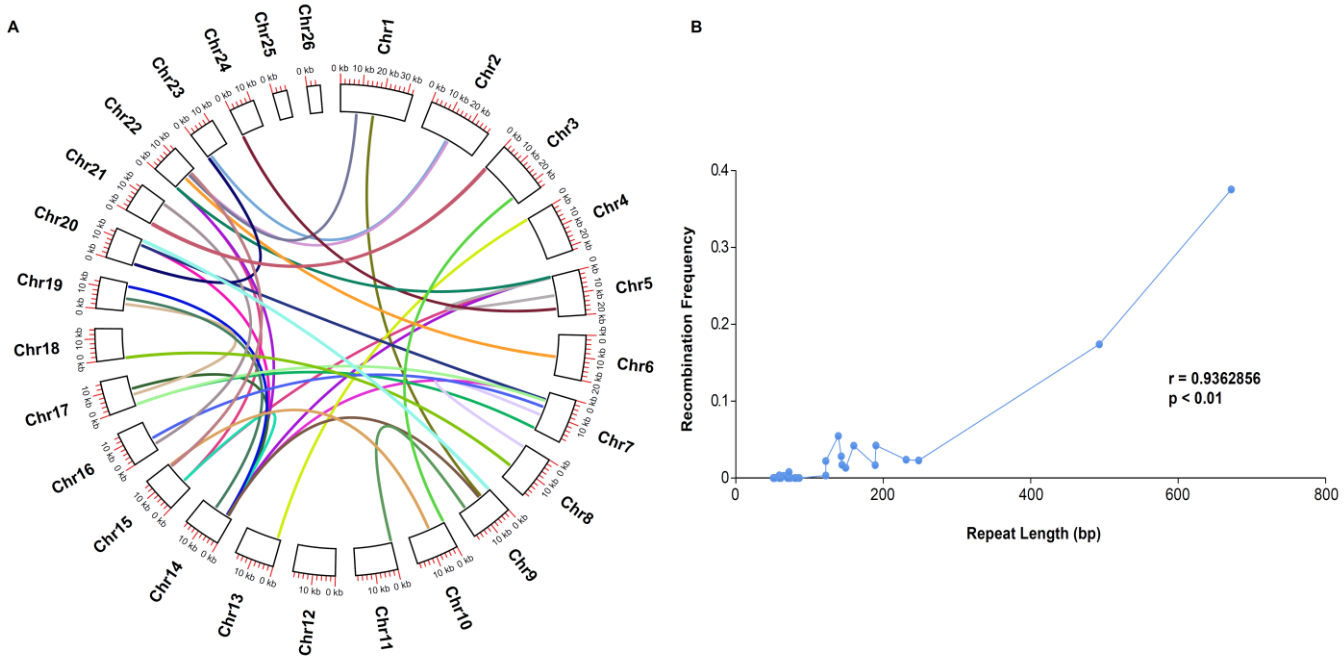

Figure 4. Recombination frequency in the mitogenome of *Paphiopedilum micranthum*. (**A**) The distribution of the 34 pairs of repeats; (**B**) recombination frequency of 34 pairs of repeats (>50 bp) with 100% identity.

3. Discussion

3.1. General Features of the P. micranthum Mitogenome

The mitogenome of *P. micranthum* was conserved in gene number and gene content compared to other angiosperm mitogenomes, encoding for 39 of the 41 protein-coding genes present in the common ancestors of angiosperms [47]—except for *sdh3* and *rpl10*, which were lost from the mitogenome of *P. micranthum* (Figure 2). *Sdh3* and *sdh4* encoded succinate dehydrogenase, and the two genes had been lost repeatedly in the mitogenomes of angiosperm [39]. While, in many other angiosperm lineages, both *sdh3* and *sdh4* are lost from the mitogenome, *sdh4* was retained in the *P. micranthum* mitogenome. Notably, the *sdh4* in *P. micranthum* contracted to 204 bp; the contraction of *sdh4* was also observed in coconut palm (183 bp) [48], and we annotated a 222 bp of *sdh4* in *Asparagus officinalis* (MT483994). *Rpl10* has frequently been reported as lost in angiosperms [24] and pseudogenized or lost in sequenced monocots [49].

The mitogenome of *P. micranthum* and *G. elata* shared 18% (about 81 kb) of their mitochondrial DNA (mtDNA) sequences, including 37 protein-coding genes (33,817 bp), and 47,121 bp non-coding regions (Figure 5). The amount of shared mtDNA was relatively small compared to most other pairs of species in seed plants [50,51]. Compared to the mitogenome of *G. elata*, the gene content of the two species was quite similar, and even the length of the cis-splicing introns was similar (Table S4). The GC content of the 26 chromosomes of *P. micranthum* was more variable compared to the 19 chromosomes of *G. elata.* Owing to active recombination, the ancestral gene clusters conserved across angiosperms were lost in *P. micranthum*; only 8 of the 14 gene clusters conserved across angiosperms were preserved. Even the two gene clusters, *nad9-trnY(GUA)* and *trnI(CAU)-trnD(GUC)*, restricted to monocots, broke in the *P. micranthum* mitogenome. Further, there were eight gene clusters shared between the mitogenome of *P. micranthum* and *G. elata*, including *atp4-ndh4L*, *rpl2-rps19-rps3-rpl16*, *rpl5-rps14-cob*, *rps13-nad1*.x2.x3, *trnY(GUA)-nad2.x*3.x4.x5, *matR-nad1.x1*, *atp1-ccmFn*,

and *apt9-rps7*; the first five of them were conserved in most angiosperms, the other three were newly formed, and *atp1-ccmFn* was restricted to Orchidaceae.

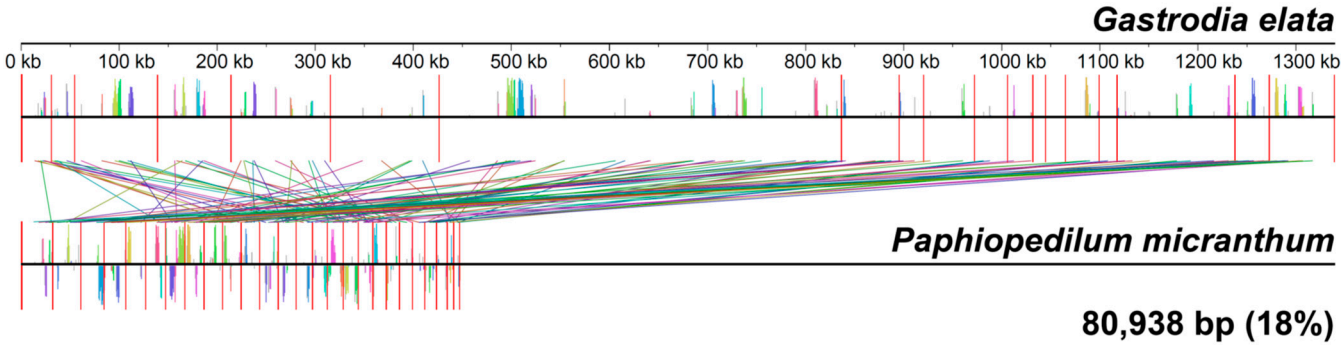

Figure 5. The colinear analysis of the mitogenome of *Paphiopedilum micranthum* and *Gastrodia elata*.

Five of the six trans-splicing introns (nad1i394, nad1i669, nad2i542, nad5i1455, and nad5i1477) were shared with the common ancestors of seed plants [24]. The trans-splicing of nad1i728 (the fourth intron) was sporadically distributed among angiosperms [24,52], and most of the species sequenced in monocots presented trans-splicing of this intron, e.g., *Allium cepa* [53] and *A. officinalis* [54], which indicates rampant recombination in the mitogenome evolution. In the *P. micranthum* mitogenome, the trans-splicing of nad1i728 was owed to the chromosome fragmentation, and exon4 and exon5 of nad1 were located in Chr7 and Chr5, respectively. Guo et al. [52] indicated that cis- shift to trans-splicing correlated with the rearrangement in the seed plants. The intrachromosomal trans-splicing to interchromosomal trans-splicing also indicates active recombination in the mitogenome.

3.2. Rampant Plastome Origin Sequences in the Mitogenome of P. micranthum

The plastome origin sequences accounted for 0.1% to 10.3% of the mitochondrial genome [47,55]. For instance, the plastome-derived sequence accounted for 1.98% (11,281 bp) in *Hibiscus cannabinus* [56], 1.16% (8937 bp) to 4.05% (37,483 bp) in kiwifruit [57], 6% (23 kb) in *Citrullus lanatus* [58], and 8.8% in vitis [59]. Further, the plastome-obtained sequences covered less than 5% of most angiosperm mitogenomes [55]. In contrast, 15 of the 26 chromosomes in the *P. micranthum* mitogenome contained plastome-derived fragments, covering 10.34% (~46 kb) of the *P. micranthum* mitogenome (Figure 3, Table 3). Compared to most other reported plastome-derived mitogenome fragments [44,60,61], the plastome-derived sequences in the mitogenome of *P. micranthum* were more pervasive and widespread, both in relative and absolute terms. The plastome-derived sequences in Chr1 even reached 12 kb (38% of Chr1) (Table 3). More than half (27,420 bp, 59%) of the plastome-origin mitogenome sequences were identical to the plastome of *P. micranthum*, with a range in size from 50 to 676 bp (Table 3). These properties suggest that the plastome-derived sequences stem from multiple transfer events, and following their intracellular transfer, these sequences experience multi-rounds of recombination.

Interestingly, *ndh* genes experienced different extents of degradation in the plastome of *Paphiopedilum*, and *ndhE*, *ndhF*, and *ndhH* have been lost from the plastome of *P. micranthum* [62]. However, the pseudo copies of ψ*ndhE*, ψ*ndhF*, and ψ*ndhH* were detected in *P. micranthum* mitogenome (Figure 1, Tables 2 and 3). Additionally, *ndhJ* was reported as a pseudogene in the plastome of *P. micranthum* owing to the non-triplet, insertion-induced, premature-stop codons [62], whereas the mitogenome of *P. micranthum* encoded the potential functional copy of *ndhJ*. These data suggest that the transfer events of *ndh* genes predated the degradation of *ndh* in the *P. micranthum* plastome, or there was more than one donor of their plastome origin sequences. Furthermore, most of the plastome origin genes have been nonfunctional pseudogenes in previous studies [3,4,40,42], except for a few cases—for instance, *psaA*, *ndhB*, and *rps7* in *H. cannabinus* [56] and *petN*, *psaA*, *atpI*, *trnI-CAU*, and *trnC-GCA* in *Mangifera* [63]. The mitogenome of *P. micranthum* contained

44 genes from plastid origin, and 12 of these genes are intact and potentially functional (*ycf4*, *cemA*, *petA*, *rbcL*, *rpoA*, *rpl36*, *ndhJ*, *psbE*, *psbF*, *psbJ*, *psbL*, and *atpE*), which has been rather rare in previous studies (Tables 2 and 3).

3.3. The Multichromosomal Mitogenome Structure of *P. micranthum*

The mitogenome of *P. micranthum* fragmented into 26 minicircular genomes (5973 bp to 32,281 bp). The mitogenome size of other species with multichromosomal structures varied widely, from 66 kb in *V. scurruloideum* [8] to 11,318 kb in *S. conica* [9], and most of these angiosperm species had two to five contigs [17], except *Cynomorium* [64] *Fagopyrum esculentum* [65], *G. elata* [37], *Geranium brycei* [40], *Lophophytum mirabile* [16], *Ombrophytum subterraneum* [12], *Rhopalocnemis phalloides* [19], and *Silene* [9,66] (Table S6). Compared to most other species with multichromosomal structures, the mitogenome of *P. micranthum* showed a more compact and fragmented genome structure. Notably, the shortest mitogenome of *P. micranthum* was 5973 bp encoding *atp8* and partially ψ*ycf1*; the size of the smallest chromosome was similar to the other species with multichromosomal structures, e.g., *O. subterraneum* (4900 bp) [12] and *R. phalloides* (4949 bp) [19]. The mitogenome fragmentation may facilitate the recombination between physically unlinked loci [66,67]. Further, 9 of the 26 chromosomes were autonomous chromosomes; these chromosomes did not contain repeats longer than 100 bp, and all the autonomous chromosomes in *P. micranthum* contained protein-coding genes, while the autonomous chromosomes in cucumber and *Silene* do not contain identifiable genes [9,15].

Repeat sequences are a source of constant rearrangement in the mitogenome [14,68–70]. Direct repeat-mediated recombination has been documented in previous studies, e.g., *Brassica campestris* [71] and *Scutellaria tsinyunensis* [27]. Li et al. [27] reported a pair of direct repeats (175 bp) mediated recombination in the mitogenome of *S. tsinyunensis*, and the 354,073 bp master circle was fragmented into two chromosomes with a length of 255,741 bp and 98,402 bp. According to the conventional multipartite model, large repeats in the master circle induced intragenomic recombination, resulting in a set of subgenomic circles [14]. Chr5 was fragmented into Chr5A and Chr5B due to a pair of 122 bp repeats (Figure S1). However, we did not detect the master circle that included the entire sequence of the *P. micranthum* mitogenome. Notably, *P. micranthum* had fewer repeat sequences, both in number and relative percentage compared to other monocot species tested [5]. Further, the number of repeat sequences (2%) was relatively less than most other species, e.g., *Mangifera* (3.5% to 4.5%) [63], *Monsonia* (3.9% to 6.9%) [68], *Trifolium* (6.6% to 8.6%) [72], and *Silene vulgaris* (18.8 to 28%) [69].

Long-read sequencing provided a reliable method to explore repeat-mediated homologous recombination. Though the mitogenome of *P. micranthum* does not contain repeats longer than 1 kb, we found alternative conformations that coexisted in the flanking regions of repeat sequences. Further, the repeat length was strongly correlated with the recombination frequency (r = 0.9379) (Figure 4, Table S5), which has also been identified in previous studies [8,9,73]. The mitogenome of *P. micranthum* was depicted as 26 minicircles for simplicity. In fact, long-read sequencing implied that the mitogenome of *P. micranthum* consisted of a population of alternative structures that resulted from dispersed repeats. Moreover, repeat sequences might play an important role in the mitogenome fragmentation of Orchidaceae.

4. Materials and Methods

4.1. Genome Sequencing, Assembly, and Annotation

We collected two fresh leaf samples of *P. micranthum* from the National Orchid Conservation and Research Center of Shenzhen (NOCC). Total genomic DNA was extracted using the cetyltrimethyl ammonium bromide (CTAB) method [74]. The extracted total genomic DNA was used for library construction with 350 bp and 20 kb insert sizes and then sequenced on MGI2000 (MGI, Shenzhen, China) and PacBio RS-II platforms (Pacific Biosciences, Menlo Park, CA, USA) for short and long reads, respectively.

The long reads were error-corrected using Canu v2.0 [75]. Then, we used the mitogenome sequences, downloaded from GenBank, as reference sequences. The potential mitogenome long reads were filtered with BLASR v5.1 [76]; short reads were filtered with a perl script described in Wang, et al. [77], and the enriched reads were used for hybrid assembly in SPAdes v3.14.1 [78]. Mitogenome contigs were filtered using BLASTN [79] and used as reference sequences for further analysis. We repeated the above steps for multiple rounds in SPAdes to improve the assembly.

In parallel, we used the complete, uncorrected datasets to assemble the mitogenome with an unpublished hybrid assembly version of NOVOPlasty [80,81]. As a seed-and-extend assembler, it needs a mitochondrial seed to initiate the assembly. Since this mitogenome exists out of multiple circular genomes, we selected all the protein-coding genes shared among angiosperms as seed sequences. Furthermore, we used the mitochondrial contigs from the SPAdes assembly that were devoid of genes as additional seeds. The overlapped regions of the above-described methods are identical, and contigs obtained from SPAdes usually lost some parts of the circular genome. In addition, we mapped the long PacBio reads to these contigs to verify the results and we de novo assembled the lost genes (*rpl10* and *sdh3*) with NOVOPlasty to confirm their absence.

The assembled contigs were annotated in Geneious Prime (Biomatters, Inc., Auckland, New Zealand) with *L. tulipifera* [23], *G. elata* [37], *A. cepa* [53], and *A. officinalis as references* [54], and refined manually. Open reading frames (ORFs) were predicted and annotated using ORFfinder in Geneious Prime, starting with ATG and of length > 300 bp. tRNA genes were annotated using tRNAscan-SE v2.0 [82]. The obtained contigs were deposited in GenBank under accession numbers OP465200–OP465225 (Table 1). The genome maps were generated with OrganellarGenomeDRAW [83]. Additionally, we used PREPACT 3.12.0 [84] to predict RNA editing in three genes (*atp6*, *atp9*, and *sdh4*) reference to *Amborella* and *Liriodendron*.

4.2. Identification of Plastid-Derived Regions and Other Horizontally Derived Regions

Firstly, the mitogenome of *P. micranthum* was searched against the plastomes of *P. micranthum* (MN587791) [62] and *C. tibeticum* (MT937101) [85] to identify plastid-derived fragments with BLAST v2.11.0+ [79], using a word size of seven, an E-value cutoff of 1×10^{-6}, and a length > 100 bp. The paralogs in the mitogenomes and plastomes were excluded from the results (e.g., *atp*1/*atp*A, *rrn*26/*rrn*23, and *rrn*18/*rrn*16), following the procedures in Guo et al. [51]. Additionally, we compared the mitochondrial homologs with putative plastid regions to evaluate the mutations in the plastid-derived mitochondrial genes. Then, we use the mitogenome of *Ustilago maydis* as reference sequences to identify the horizontal gene transfer fragments mentioned in Sinn and Barrett [31].

4.3. Repeat and Repeats-Mediated Homologous Recombinations

Tandem repeats in the *P. micranthum* mitogenome were identified using Tandem Repeat Finder v4.09 [86] with default parameters. The dispersed repeats were detected using the python tool ROUSFinder.py [5] with a minimum repeat size of 50 bp. Then, we calculated the recombination frequency of 34 pairs of repeats with 100% identity, following the methods of Sullivan et al. [70]. For each repeat pair, we extracted ±2000 bp flanking regions and constructed two potentially alternative conformations. The recombination rate was calculated by dividing the number of recombinant reads by the total number of reads spanning each repeat. In addition, we tested whether the repeat length correlated with the recombination frequency.

5. Conclusions

We accurately assembled the mitogenome of *P. micranthum* with a combination of long- and short-read data. The mitogenome of *P. micranthum* presents typical multichromosomal structures and preserves a large amount of plastome-derived horizontal gene transfer fragments. Considering the genome size and chromosome number, the mitogenome of *P. micranthum* is more fragmented than most other species with multichromosomal genome

structures. The long reads provide strong evidence for the plastome-to-mitogenome intracellular gene transfer and the repeat-mediated homologous recombination. The comparison of the *P. micranthum* mitogenome with the mitogenome of *G. elata* sheds light on the mitogenome evolution of Orchidaceae. Though the mitogenomes of the two species have similar gene content, the mitogenomes of the two species share only 81 kb of their mtDNA sequence. Considering the disparities in genome size and chromosome number, the high frequency of recombination, intraspecies genome structure variation, and the low collinearity of the two orchids, our understanding of the mitogenome evolution of orchids is rather limited. Further studies are needed to unravel the mitogenome evolution of orchids.

Supplementary Materials: The following are available online at https://www.mdpi.com/article/10.3390/ijms24043976/s1.

Author Contributions: Conceptualization, Y.-Y.G.; data curation, J.-X.Y. and Y.-Y.G.; formal analysis, J.-X.Y., N.D. and M.-Z.B.; funding acquisition, Y.-Y.G. and N.D.; methodology, Y.-Y.G.; resources, Y.-Y.G.; software, J.-X.Y. and N.D.; writing—original draft, J.-X.Y. and Y.-Y.G.; writing—review and editing, N.D. and Y.-Y.G. All authors have read and agreed to the published version of the manuscript.

Funding: This research was funded by the National Natural Science Foundation of China (grant number U1804117 to Y.-Y.G.) and KU Leuven (postdoctoral mandate PDMT1/21/033 to N.D.)

Institutional Review Board Statement: Not applicable.

Informed Consent Statement: Not applicable.

Data Availability Statement: The annotated mitogenomes generated in this study are deposited in GenBank under accession Nos. OP465200–OP465225.

Acknowledgments: The authors thank the Editor and the anonymous reviewers for their insightful comments and suggestions on the manuscript. The authors thank Guo-Qiang Zhang for help with sample collection and Fu-Chao Guo for help in the analysis of RNA editing.

Conflicts of Interest: The authors declare no conflict of interest.

References

1. Palmer, J.D.; Herbon, L.A. Plant mitochondrial DNA evolved rapidly in structure, but slowly in sequence. *J. Mol. Evol.* **1988**, *28*, 87–97. [CrossRef] [PubMed]
2. Bergthorsson, U.; Adams, K.; Thomason, B.; Palmer, J. Widespread horizontal transfer of mitochondrial genes in flowering plants. *Nature* **2003**, *424*, 197–201. [CrossRef]
3. Rice, D.W.; Alverson, A.J.; Richardson, A.O.; Young, G.J.; Sanchez-Puerta, M.V.; Munzinger, J.; Barry, K.; Boore, J.L.; Zhang, Y.; dePamphilis, C.W.; et al. Horizontal transfer of entire genomes via mitochondrial fusion in the angiosperm *Amborella*. *Science* **2013**, *342*, 1468–1473. [CrossRef] [PubMed]
4. Mower, J.P.; Jain, K.; Hepburn, N.J. The Role of Horizontal Transfer in Shaping the Plant Mitochondrial Genome. In *Mitochondrial Genome Evolution*; Maréchal-Drouard, L., Ed.; Academic Press: Berkeley, CA, USA, 2012; Volume 63, pp. 41–69.
5. Wynn, E.L.; Christensen, A.C. Repeats of unusual size in plant mitochondrial genomes: Identification, incidence and evolution. *G3-GENES GENOM GENET* **2019**, *9*, 549–559. [CrossRef] [PubMed]
6. Small, I.D.; Schallenberg-Rüdinger, M.; Takenaka, M.; Mireau, H.; Ostersetzer-Biran, O. Plant organellar RNA editing: What 30 years of research has revealed. *Plant J.* **2020**, *101*, 1040–1056. [CrossRef] [PubMed]
7. Knoop, V. C-to-U and U-to-C: RNA editing in plant organelles and beyond. *J. Exp. Bot.* **2022**, erac488. [CrossRef]
8. Skippington, E.; Barkman, T.J.; Rice, D.W.; Palmer, J.D. Miniaturized mitogenome of the parasitic plant *Viscum scurruloideum* is extremely divergent and dynamic and has lost all *nad* genes. *Proc. Natl. Acad. Sci. USA* **2015**, *112*, E3515–E3524. [CrossRef]
9. Sloan, D.B.; Alverson, A.J.; Chuckalovcak, J.P.; Wu, M.; McCauley, D.E.; Palmer, J.D.; Taylor, D.R. Rapid evolution of enormous, multichromosomal genomes in flowering plant mitochondria with exceptionally high mutation rates. *PLoS Biol.* **2012**, *10*, e1001241. [CrossRef]
10. Backert, S.; Nielsen, B.L.; Börner, T. The mystery of the rings: Structure and replication of mitochondrial genomes from higher plants. *Trends Plant Sci.* **1997**, *2*, 477–483. [CrossRef]
11. Kozik, A.; Rowan, B.A.; Lavelle, D.; Berke, L.; Schranz, M.E.; Michelmore, R.W.; Christensen, A.C. The alternative reality of plant mitochondrial DNA: One ring does not rule them all. *PLoS Genet.* **2019**, *15*, e1008373. [CrossRef]
12. Roulet, M.E.; Garcia, L.E.; Gandini, C.L.; Sato, H.; Ponce, G.; Sanchez-Puerta, M.V. Multichromosomal structure and foreign tracts in the *Ombrophytum subterraneum* (Balanophoraceae) mitochondrial genome. *Plant Mol. Biol.* **2020**, *103*, 623–638. [CrossRef] [PubMed]

13. Gualberto, J.M.; Newton, K.J. Plant mitochondrial genomes: Dynamics and mechanisms of mutation. *Annu. Rev. Plant Biol.* **2017**, *68*, 225–252. [CrossRef] [PubMed]
14. Sloan, D.B. One ring to rule them all? Genome sequencing provides new insights into the 'master circle' model of plant mitochondrial DNA structure. *New Phytol.* **2013**, *200*, 978–985. [CrossRef] [PubMed]
15. Alverson, A.J.; Rice, D.W.; Dickinson, S.L.; Barry, K.; Palmer, J.D. Origins and recombination of the bacterial-sized multichromosomal mitochondrial genome of cucumber. *Plant Cell* **2011**, *23*, 2499–2513. [CrossRef]
16. Sanchez-Puerta, M.V.; García, L.E.; Wohlfeiler, J.; Ceriotti, L.F. Unparalleled replacement of native mitochondrial genes by foreign homologs in a holoparasitic plant. *New Phytol.* **2017**, *214*, 376–387. [CrossRef]
17. Wu, Z.-Q.; Liao, X.-Z.; Zhang, X.-N.; Tembrock, L.R.; Broz, A. Genomic architectural variation of plant mitochondria—A review of multichromosomal structuring. *J. Syst. Evol.* **2022**, *60*, 160–168. [CrossRef]
18. Varré, J.-S.; D'Agostino, N.; Touzet, P.; Gallina, S.; Tamburino, R.; Cantarella, C.; Ubrig, E.; Cardi, T.; Drouard, L.; Gualberto, J.M. Complete sequence, multichromosomal architecture and transcriptome analysis of the *Solanum tuberosum* mitochondrial genome. *Int. J. Mol. Sci.* **2019**, *20*, 4788. [CrossRef]
19. Yu, R.; Sun, C.; Zhong, Y.; Liu, Y.; Sanchez-Puerta, M.V.; Mower, J.P.; Zhou, R. The minicircular and extremely heteroplasmic mitogenome of the holoparasitic plant *Rhopalocnemis phalloides*. *Curr. Biol.* **2022**, *32*, 470–479.e5. [CrossRef]
20. Zhu, A.; Guo, W.; Jain, K.; Mower, J.P. Unprecedented heterogeneity in the synonymous substitution rate within a plant genome. *Mol. Biol. Evol.* **2014**, *31*, 1228–1236. [CrossRef]
21. Liu, F.; Fan, W.; Yang, J.-B.; Xiang, C.-L.; Mower, J.P.; Li, D.-Z.; Zhu, A. Episodic and guanine–cytosine-biased bursts of intragenomic and interspecific synonymous divergence in Ajugoideae (Lamiaceae) mitogenomes. *New Phytol.* **2020**, *228*, 1107–1114. [CrossRef]
22. Cho, Y.; Mower, J.P.; Qiu, Y.L.; Palmer, J.D. Mitochondrial substitution rates are extraordinarily elevated and variable in a genus of flowering plants. *Proc. Natl. Acad. Sci. USA* **2004**, *101*, 17741–17746. [CrossRef]
23. Richardson, A.O.; Rice, D.W.; Young, G.J.; Alverson, A.J.; Palmer, J.D. The "fossilized" mitochondrial genome of *Liriodendron tulipifera*: Ancestral gene content and order, ancestral editing sites, and extraordinarily low mutation rate. *BMC Biol.* **2013**, *11*, 29. [CrossRef]
24. Mower, J.P. Variation in protein gene and intron content among land plant mitogenomes. *Mitochondrion* **2020**, *53*, 203–213. [CrossRef] [PubMed]
25. Dong, S.; Zhao, C.; Chen, F.; Liu, Y.; Zhang, S.; Wu, H.; Zhang, L.; Liu, Y. The complete mitochondrial genome of the early flowering plant *Nymphaea colorata* is highly repetitive with low recombination. *BMC Genom.* **2018**, *19*, 614. [CrossRef] [PubMed]
26. Liu, H.; Yu, J.; Yu, X.; Zhang, D.; Chang, H.; Li, W.; Song, H.; Cui, Z.; Wang, P.; Luo, Y.; et al. Structural variation of mitochondrial genomes sheds light on evolutionary history of soybeans. *Plant J.* **2021**, *108*, 1456–1472. [CrossRef]
27. Li, J.; Xu, Y.; Shan, Y.; Pei, X.; Yong, S.; Liu, C.; Yu, J. Assembly of the complete mitochondrial genome of an endemic plant, *Scutellaria tsinyunensis*, revealed the existence of two conformations generated by a repeat-mediated recombination. *Planta* **2021**, *254*, 36. [CrossRef] [PubMed]
28. Li, J.; Cullis, C. The multipartite mitochondrial genome of marama (*Tylosema esculentum*). *Front. Plant Sci.* **2021**, *12*, 787443. [CrossRef]
29. Dong, S.; Zhao, C.; Zhang, S.; Zhang, L.; Wu, H.; Liu, H.; Zhu, R.; Jia, Y.; Goffinet, B.; Liu, Y. Mitochondrial genomes of the early land plant lineage liverworts (Marchantiophyta): Conserved genome structure, and ongoing low frequency recombination. *BMC Genom.* **2019**, *20*, 953. [CrossRef]
30. Kang, J.S.; Zhang, H.R.; Wang, Y.R.; Liang, S.Q.; Mao, Z.Y.; Zhang, X.C.; Xiang, Q.P. Distinctive evolutionary pattern of organelle genomes linked to the nuclear genome in Selaginellaceae. *Plant J.* **2020**, *104*, 1657–1672. [CrossRef]
31. Sinn, B.T.; Barrett, C.F. Ancient mitochondrial gene transfer between fungi and the orchids. *Mol. Biol. Evol.* **2020**, *37*, 44–57. [CrossRef]
32. Kinkar, L.; Gasser, R.B.; Webster, B.L.; Rollinson, D.; Littlewood, D.T.J.; Chang, B.C.; Stroehlein, A.J.; Korhonen, P.K.; Young, N.D. Nanopore sequencing resolves elusive long tandem-repeat regions in mitochondrial genomes. *Int. J. Mol. Sci.* **2021**, *22*, 1811. [CrossRef] [PubMed]
33. Achakkagari, S.R.; Tai, H.H.; Davidson, C.; De Jong, H.; Strömvik, M.V. The complete mitogenome assemblies of 10 diploid potato clones reveal recombination and overlapping variants. *DNA Res.* **2021**, *28*, dsab009. [CrossRef] [PubMed]
34. Sathiyadash, K.; Muthukumar, T.; Karthikeyan, V.; Rajendran, K. Orchid Mycorrhizal Fungi: Structure, Function, and Diversity. In *Orchid Biology: Recent Trends & Challenges*; Khasim, S., Hegde, S., González-Arnao, M., Thammasiri, K., Eds.; Springer: Singapore, 2020; pp. 239–280.
35. Rasmussen, H.N. *Terrestrial orchids: From Seed to Mycotrophic Plant*; Cambridge University Press: Cambridge, UK, 1995.
36. Jacquemyn, H.; Merckx, V.S. Mycorrhizal symbioses and the evolution of trophic modes in plants. *J. Ecol.* **2019**, *107*, 1567–1581. [CrossRef]
37. Yuan, Y.; Jin, X.; Liu, J.; Zhao, X.; Zhou, J.; Wang, X.; Wang, D.; Lai, C.; Xu, W.; Huang, J. The *Gastrodia elata* genome provides insights into plant adaptation to heterotrophy. *Nat. Commun.* **2018**, *9*, 1615. [CrossRef]
38. Zhao, N.; Wang, Y.; Hua, J. The roles of mitochondrion in intergenomic gene transfer in plants: A source and a pool. *Int. J. Mol. Sci.* **2018**, *19*, 547. [CrossRef]
39. Adams, K.L.; Qiu, Y.L.; Stoutemyer, M.; Palmer, J.D. Punctuated evolution of mitochondrial gene content: High and variable rates of mitochondrial gene loss and transfer to the nucleus during angiosperm evolution. *Proc. Natl. Acad. Sci. USA* **2002**, *99*, 9905–9912. [CrossRef]
40. Park, S.; Grewe, F.; Zhu, A.; Ruhlman, T.A.; Sabir, J.; Mower, J.P.; Jansen, R.K. Dynamic evolution of *Geranium* mitochondrial genomes through multiple horizontal and intracellular gene transfers. *New Phytol.* **2015**, *208*, 570–583. [CrossRef]

41. Choi, I.-S.; Wojciechowski, M.F.; Ruhlman, T.A.; Jansen, R.K. In and out: Evolution of viral sequences in the mitochondrial genomes of legumes (Fabaceae). *Mol. Phylogenet. Evol.* **2021**, *163*, 107236. [CrossRef]
42. Warren, J.M.; Sloan, D.B. Interchangeable parts: The evolutionarily dynamic tRNA population in plant mitochondria. *Mitochondrion* **2020**, *52*, 144–156. [CrossRef]
43. Garcia, L.E.; Edera, A.A.; Palmer, J.D.; Sato, H.; Sanchez-Puerta, M.V. Horizontal gene transfers dominate the functional mitochondrial gene space of a holoparasitic plant. *New Phytol.* **2021**, *229*, 1701–1714. [CrossRef]
44. Choi, K.-S.; Park, S. Complete plastid and mitochondrial genomes of *Aeginetia indica* reveal Intracellular Gene Transfer (IGT), Horizontal Gene Transfer (HGT), and Cytoplasmic Male Sterility (CMS). *Int. J. Mol. Sci.* **2021**, *22*, 6143. [CrossRef] [PubMed]
45. Mower, J.P.; Stefanovi, S.; Hao, W.; Gummow, J.S.; Jain, K.; Ahmed, D.; Palmer, J.D. Horizontal acquisition of multiple mitochondrial genes from a parasitic plant followed by gene conversion with host mitochondrial genes. *BMC Biol.* **2010**, *8*, 150. [CrossRef]
46. Liu, Z.; Chen, S.; Chen, L.; Lei, S. *The Genus Paphiopedilum in China*; Science Press: Beijing, China, 2009.
47. Mower, J.P.; Sloan, D.B.; Alverson, A.J. Plant Mitochondrial Genome Diversity: The Genomics Revolution. In *Plant Genome Diversity Volume 1: Plant Genomes, Their Residents, and Their Evolutionary Dynamics*; Wendel, J.F., Greilhuber, J., Dolezel, J., Leitch, I.J., Eds.; Springer: Vienna, Austria, 2012; pp. 123–144.
48. Aljohi, H.A.; Liu, W.; Lin, Q.; Zhao, Y.; Zeng, J.; Alamer, A.; Alanazi, I.O.; Alawad, A.O.; Al-Sadi, A.M.; Hu, S. Complete sequence and analysis of coconut palm (*Cocos nucifera*) mitochondrial genome. *PLoS ONE* **2016**, *11*, e0163990. [CrossRef] [PubMed]
49. Mower, J.P.; Bonen, L. Ribosomal protein L10 is encoded in the mitochondrial genome of many land plants and green algae. *BMC Evol. Biol.* **2009**, *9*, 265. [CrossRef] [PubMed]
50. Shi, Y.; Liu, Y.; Zhang, S.; Zou, R.; Tang, J.; Mu, W.; Peng, Y.; Dong, S. Assembly and comparative analysis of the complete mitochondrial genome sequence of *Sophora japonica* 'JinhuaiJ2'. *PLoS ONE* **2018**, *13*, e0202485. [CrossRef] [PubMed]
51. Guo, W.; Grewe, F.; Fan, W.; Young, G.J.; Knoop, V.; Palmer, J.D.; Mower, J.P. Ginkgo and Welwitschia mitogenomes reveal extreme contrasts in gymnosperm mitochondrial evolution. *Mol. Biol. Evol.* **2016**, *33*, 1448–1460. [CrossRef] [PubMed]
52. Guo, W.; Zhu, A.; Fan, W.; Adams, R.P.; Mower, J.P. Extensive shifts from cis-to trans-splicing of gymnosperm mitochondrial introns. *Mol. Biol. Evol.* **2020**, *37*, 1615–1620. [CrossRef]
53. Kim, B.; Kim, K.; Yang, T.-J.; Kim, S. Completion of the mitochondrial genome sequence of onion (*Allium cepa* L.) containing the CMS-S male-sterile cytoplasm and identification of an independent event of the *ccmFN* gene split. *Curr. Genet.* **2016**, *62*, 873–885. [CrossRef]
54. Sheng, W. The complete mitochondrial genome of *Asparagus officinalis* L. *Mitochondrial DNA B Resour.* **2020**, *5*, 2627–2628. [CrossRef]
55. Sloan, D.B.; Wu, Z. History of plastid DNA insertions reveals weak deletion and AT mutation biases in angiosperm mitochondrial genomes. *Genome Biol. Evol.* **2014**, *6*, 3210–3221. [CrossRef]
56. Liao, X.; Zhao, Y.; Kong, X.; Khan, A.; Zhou, B.; Liu, D.; Kashif, M.H.; Chen, P.; Wang, H.; Zhou, R. Complete sequence of kenaf (*Hibiscus cannabinus*) mitochondrial genome and comparative analysis with the mitochondrial genomes of other plants. *Sci. Rep.* **2018**, *8*, 12714. [CrossRef] [PubMed]
57. Wang, S.; Li, D.; Yao, X.; Song, Q.; Wang, Z.; Zhang, Q.; Zhong, C.; Liu, Y.; Huang, H. Evolution and diversification of kiwifruit mitogenomes through extensive whole-genome rearrangement and mosaic loss of intergenic sequences in a highly variable region. *Genome Biol. Evol.* **2019**, *11*, 1192–1206. [CrossRef] [PubMed]
58. Alverson, A.J.; Wei, X.X.; Rice, D.W.; Stern, D.B.; Barry, K.; Palmer, J.D. Insights into the evolution of mitochondrial genome size from complete sequences of *Citrullus lanatus* and *Cucurbita pepo* (Cucurbitaceae). *Mol. Biol. Evol.* **2010**, *27*, 1436–1448. [CrossRef] [PubMed]
59. Goremykin, V.V.; Salamini, F.; Velasco, R.; Viola, R. Mitochondrial DNA of Vitis vinifera and the issue of rampant horizontal gene transfer. *Mol. Biol. Evol.* **2009**, *26*, 99–110. [CrossRef]
60. Gandini, C.; Sanchez-Puerta, M. Foreign plastid sequences in plant mitochondria are frequently acquired via mitochondrion-to-mitochondrion horizontal transfer. *Sci. Rep.* **2017**, *7*, 43402. [CrossRef]
61. Fang, Y.; Wu, H.; Zhang, T.; Yang, M.; Yin, Y.; Pan, L.; Yu, X.; Zhang, X.; Hu, S.; Al-Mssallem, I.S. A complete sequence and transcriptomic analyses of date palm (*Phoenix dactylifera* L.) mitochondrial genome. *PLoS ONE* **2012**, *7*, e37164. [CrossRef]
62. Guo, Y.-Y.; Yang, J.-X.; Bai, M.-Z.; Zhang, G.-Q.; Liu, Z.-J. The chloroplast genome evolution of Venus slipper (*Paphiopedilum*): IR expansion, SSC contraction, and highly rearranged SSC regions. *BMC Plant Biol.* **2021**, *21*, 248. [CrossRef]
63. Niu, Y.; Gao, C.; Liu, J. Complete mitochondrial genomes of three *Mangifera* species, their genomic structure and gene transfer from chloroplast genomes. *BMC Genom.* **2022**, *23*, 147. [CrossRef]
64. Bellot, S.; Cusimano, N.; Luo, S.; Sun, G.; Zarre, S.; Gröger, A.; Temsch, E.; Renner, S.S. Assembled plastid and mitochondrial genomes, as well as nuclear genes, place the parasite family Cynomoriaceae in the Saxifragales. *Genome Biol. Evol.* **2016**, *8*, 2214–2230. [CrossRef]
65. Logacheva, M.D.; Schelkunov, M.I.; Fesenko, A.N.; Kasianov, A.S.; Penin, A.A. Mitochondrial genome of *Fagopyrum esculentum* and the genetic diversity of extranuclear genomes in buckwheat. *Plants* **2020**, *9*, 618. [CrossRef]
66. Wu, Z.; Cuthbert, J.M.; Taylor, D.R.; Sloan, D.B. The massive mitochondrial genome of the angiosperm *Silene noctiflora* is evolving by gain or loss of entire chromosomes. *Proc. Natl. Acad. Sci. USA* **2015**, *112*, 10185–10191. [CrossRef] [PubMed]
67. Rand, D.M. 'Why genomes in pieces?' revisited: Sucking lice do their own thing in mtDNA circle game. *Genome Res.* **2009**, *19*, 700–702. [CrossRef] [PubMed]
68. Cole, L.W.; Guo, W.; Mower, J.P.; Palmer, J.D. High and variable rates of repeat-mediated mitochondrial genome rearrangement in a genus of plants. *Mol. Biol. Evol.* **2018**, *35*, 2773–2785. [CrossRef] [PubMed]

69. Sloan, D.B.; Muller, K.; Mccauley, D.E.; Taylor, D.R.; Storchova, H. Intraspecific variation in mitochondrial genome sequence, structure, and gene content in *Silene vulgaris*, an angiosperm with pervasive cytoplasmic male sterility. *New Phytol.* **2012**, *196*, 1228–1239. [CrossRef]
70. Sullivan, A.R.; Eldfjell, Y.; Schiffthaler, B.; Delhomme, N.; Asp, T.; Hebelstrup, K.H.; Keech, O.; Öberg, L.; Møller, I.M.; Arvestad, L. The mitogenome of Norway spruce and a reappraisal of mitochondrial recombination in plants. *Genome Biol. Evol.* **2020**, *12*, 3586–3598. [CrossRef]
71. Palmer, J.D.; Shields, C.R. Tripartite structure of the *Brassica campestris* mitochondrial genome. *Nature* **1984**, *307*, 437–440. [CrossRef]
72. Choi, I.-S.; Ruhlman, T.A.; Jansen, R.K. Comparative mitogenome analysis of the genus *Trifolium* reveals independent gene fission of *ccmFn* and intracellular gene transfers in Fabaceae. *Int. J. Mol. Sci.* **2020**, *21*, 1959. [CrossRef]
73. Dong, S.; Chen, L.; Liu, Y.; Wang, Y.; Zhang, S.; Yang, L.; Lang, X.; Zhang, S. The draft mitochondrial genome of *Magnolia biondii* and mitochondrial phylogenomics of angiosperms. *PLoS ONE* **2020**, *15*, e0231020. [CrossRef]
74. Doyle, J.; Doyle, J. A rapid DNA isolation procedure for small quantities of fresh leaf tissue. *Phytochem. Bull.* **1987**, *19*, 11–15.
75. Koren, S.; Walenz, B.P.; Berlin, K.; Miller, J.R.; Bergman, N.H.; Phillippy, A.M. Canu: Scalable and accurate long-read assembly via adaptive k-mer weighting and repeat separation. *Genome Res.* **2017**, *27*, 722–736. [CrossRef]
76. Chaisson, M.J.; Tesler, G. Mapping single molecule sequencing reads using basic local alignment with successive refinement (BLASR): Application and theory. *BMC Bioinform.* **2012**, *13*, 238. [CrossRef] [PubMed]
77. Wang, W.; Schalamun, M.; Morales-Suarez, A.; Kainer, D.; Schwessinger, B.; Lanfear, R. Assembly of chloroplast genomes with long- and short-read data: A comparison of approaches using *Eucalyptus pauciflora* as a test case. *BMC Genom.* **2018**, *19*, 977. [CrossRef] [PubMed]
78. Bankevich, A.; Nurk, S.; Antipov, D.; Gurevich, A.A.; Dvorkin, M.; Kulikov, A.S.; Lesin, V.M.; Nikolenko, S.I.; Pham, S.; Prjibelski, A.D. SPAdes: A new genome assembly algorithm and its applications to single-cell sequencing. *J. Comput. Biol.* **2012**, *19*, 455–477. [CrossRef] [PubMed]
79. Camacho, C.; Coulouris, G.; Avagyan, V.; Ma, N.; Papadopoulos, J.; Bealer, K.; Madden, T.L. BLAST+: Architecture and applications. *BMC Bioinform.* **2009**, *10*, 421. [CrossRef]
80. Dierckxsens, N.; Mardulyn, P.; Smits, G. Unraveling heteroplasmy patterns with NOVOPlasty. *NAR Genom. Bioinform.* **2020**, *2*, lqz011. [CrossRef] [PubMed]
81. Dierckxsens, N.; Mardulyn, P.; Smits, G. NOVOPlasty: De novo assembly of organelle genomes from whole genome data. *Nucleic Acids Res.* **2017**, *45*, e18. [PubMed]
82. Chan, P.P.; Lin, B.Y.; Mak, A.J.; Lowe, T.M. tRNAscan-SE 2.0: Improved detection and functional classification of transfer RNA genes. *Nucleic Acids Res.* **2021**, *49*, 9077–9096. [CrossRef] [PubMed]
83. Greiner, S.; Lehwark, P.; Bock, R. OrganellarGenomeDRAW (OGDRAW) version 1.3. 1: Expanded toolkit for the graphical visualization of organellar genomes. *Nucleic Acids Res.* **2019**, *47*, W59–W64. [CrossRef]
84. Lenz, H.; Hein, A.; Knoop, V. Plant organelle RNA editing and its specificity factors: Enhancements of analyses and new database features in PREPACT 3.0. *BMC Bioinform.* **2018**, *19*, 255. [CrossRef]
85. Guo, Y.-Y.; Yang, J.-X.; Li, H.-K.; Zhao, H.-S. Chloroplast genomes of two species of *Cypripedium*: Expanded genome size and proliferation of AT-biased repeat sequences. *Front. Plant Sci.* **2021**, *12*, 609729. [CrossRef]
86. Benson, G. Tandem repeats finder: A program to analyze DNA sequences. *Nucleic Acids Res.* **1999**, *27*, 573–580. [CrossRef] [PubMed]